Trpc5 deficiency causes hypoprolactinemia and altered function of oscillatory dopamine neurons in the arcuate nucleus

Thomas Blum[a,1], Ana Moreno-Pérez[a,1], Martina Pyrski[a], Bernd Bufe[a,2], Anela Arifovic[a], Petra Weissgerber[b], Marc Freichel[c], Frank Zufall[a,3], and Trese Leinders-Zufall[a,3]

[a]Center for Integrative Physiology and Molecular Medicine, Saarland University, 66421 Homburg, Germany; [b]Department of Pharmacology and Toxicology, Saarland University, 66421 Homburg, Germany; and [c]Institute of Pharmacology, University of Heidelberg, 69120 Heidelberg, Germany

Edited by David Julius, University of California, San Francisco, CA, and approved June 17, 2019 (received for review April 6, 2019)

Dopamine neurons of the hypothalamic arcuate nucleus (ARC) tonically inhibit the release of the protein hormone prolactin from lactotropic cells in the anterior pituitary gland and thus play a central role in prolactin homeostasis of the body. Prolactin, in turn, orchestrates numerous important biological functions such as maternal behavior, reproduction, and sexual arousal. Here, we identify the canonical transient receptor potential channel Trpc5 as an essential requirement for normal function of dopamine ARC neurons and prolactin homeostasis. By analyzing female mice carrying targeted mutations in the *Trpc5* gene including a conditional Trpc5 deletion, we show that Trpc5 is required for maintaining highly stereotyped infraslow membrane potential oscillations of dopamine ARC neurons. Trpc5 is also required for eliciting prolactin-evoked tonic plateau potentials in these neurons that are part of a regulatory feedback circuit. Trpc5 mutant females show severe prolactin deficiency or hypoprolactinemia that is associated with irregular reproductive cyclicity, gonadotropin imbalance, and impaired reproductive capabilities. These results reveal a previously unknown role for the cation channel Trpc5 in prolactin homeostasis of female mice and provide strategies to explore the genetic basis of reproductive disorders and other malfunctions associated with defective prolactin regulation in humans.

Trpc5 channelopathy | hypothalamus | dopamine | prolactin | HC-070

The transient receptor potential (TRP) channel Trpc5 is a member of the transient receptor potential channel (TRPC) subfamily of nonselective, Ca^{2+}-permeable, and receptor-operated cation channels (1–4). Trpc5 is predominantly expressed in the central nervous system (CNS) (3), but it is also thought to play important roles in kidney function (5) and the vascular system (3). In the CNS, an essential role for Trpc5 in amygdala function and fear-related behavior has been established (6). Furthermore, Trpc5 channels are implicated in depolarization and bursting during epileptiform seizures (7) and in contributing to hippocampal growth cone (8) and synaptic function (9). Recent studies also show that Trpc5 mediates the acute effects of leptin, insulin, and serotonin in a specific subset of hypothalamic arcuate nucleus (ARC) neurons known as POMC neurons, thereby linking Trpc5 activation to energy balance, feeding behavior, and glucose metabolism (10, 11). Thus, understanding the role of Trpc5 in the CNS is fundamental for gaining insight into a wide range of brain functions, the control of innate behaviors, and systemic diseases.

We hypothesized that Trpc5 may play a critical role in a distinct subtype of neuroendocrine ARC neurons, the dopamine neurons of the tuberoinfundibular pathway (12–14). By projecting to the median eminence, these cells contribute to one of the major dopamine-signaling systems in the brain (15). Dopamine released from their axon terminals is transported to the anterior pituitary gland where it inhibits the secretion of the protein hormone prolactin from lactotropic cells (12, 16). Prolactin, in turn, influences numerous biological processes essential for successful reproduction, maternal behavior, sexual desire, metabolism, and immune system function (14, 16). During early pregnancy, a decline in dopamine release is required to elevate prolactin levels, thereby stimulating a hormonal pathway that prepares the uterine endometrium for implantation of a fertilized ovum (16). Thus, the firing properties of these neurons are likely to control the release of dopamine (17–20) and therefore should be critical to determine reproductive success. A recent report investigating dopamine release dynamics confirmed the tight relationship between impulse activity and vesicular release in the tuberoinfundibular dopamine system (21).

Here, we examine the requirement of Trpc5 for regulating circulating prolactin levels and for maintaining highly stereotyped oscillatory activity in dopaminergic ARC neurons. We also investigate the requirement of Trpc5 in the acute effects of prolactin on the excitation of these neurons. By analyzing several Trpc5-deficient mouse strains including a conditional Trpc5 deletion in tyrosine hydroxylase-expressing (Th^+) neurons—combined with

Significance

The hormone prolactin orchestrates one of the widest ranges of functions of any extracellular signaling molecule including maternal behavior, reproduction, and sexual desire. Its secretion is under inhibitory control by dopamine released from neuroendocrine cells in the hypothalamic arcuate nucleus. Hallmarks of these neurons are their infraslow oscillatory activity and their tonic excitation to acute prolactin stimulation that is necessary for feedback control. We identify the transient receptor potential cation channel Trpc5 as a crucial requirement for normal oscillations and prolactin-evoked plateau potentials in these neurons. Trpc5-deficient female mice show severe hypoprolactinemia, hormonal imbalance, and impairments in their reproductive capabilities. Thus, Trpc5 occupies a critical position in hypothalamic neurons controlling prolactin regulation in the body.

Author contributions: T.B., A.M.-P., M.P., B.B., F.Z., and T.L.-Z. designed research; T.B., A.M.-P., M.P., B.B., A.A., and T.L.-Z. performed research; P.W., M.F., and T.L.-Z. contributed new reagents/analytic tools; T.B., A.M.-P., M.P., B.B., A.A., F.Z., and T.L.-Z. analyzed data; M.P. and B.B. contributed to the writing of the manuscript; and F.Z. and T.L.-Z. wrote the paper.

The authors declare no conflict of interest.

This article is a PNAS Direct Submission.

Data deposition: The datasets generated and/or analyzed during the present study have been deposited in Figshare (https://doi.org/10.6084/m9.figshare.8325569).

[1]T.B. and A.M.-P. contributed equally to this work.

[2]Present address: Immunology Section, Faculty of Computer Science and Microsystems Engineering, University of Applied Sciences Kaiserslautern, 66482 Zweibrücken, Germany.

[3]To whom correspondence may be addressed. Email: frank.zufall@uks.eu or trese.leinders@uks.eu.

This article contains supporting information online at www.pnas.org/lookup/suppl/doi:10.1073/pnas.1905705116/-/DCSupplemental.

Published online July 8, 2019.

acute pharmacological treatment using the potent Trpc5 antagonist HC-070 (22) and synaptic uncoupling—we discovered that Trpc5 is critical for maintaining infraslow membrane potential oscillations and for mediating long-lasting plateau potentials to prolactin exposure in dopaminergic ARC neurons. We also found that Trpc5 deficiency causes profound hypoprolactinemia that is associated with irregular reproductive cyclicity, gonadotropin imbalance, and impaired reproductive capabilities. Thus, Trpc5 is a major determinant of hypothalamic prolactin regulation and defines the functional properties of dopaminergic ARC neurons that play a central role in prolactin homeostasis.

Results

Trpc5 Is Expressed in Th$^+$ Neurons of the Arcuate Nucleus. To investigate expression of Trpc5 in dopamine neurons of mouse ARC, we performed double-labeling immunohistochemistry using specific antibodies that recognize Th and Trpc5 (Fig. 1 *A–C*). We used tissue from adult (6–23 wk old) female mice irrespective of estrous stage. We also analyzed genetically altered mice in which all Th$^+$ neurons (23) were identifiable through their intrinsic red fluorescence (Th-tdTomato) (24) (*SI Appendix*, Fig. S1*A*). Together, these studies revealed that the majority of Th$^+$ ARC neurons (~85%) in wild-type mice exhibit acute Trpc5 protein expression (Fig. 1 *A–C* and *SI Appendix*, Fig. S1*A*). By contrast, lactotrophs in the anterior pituitary—which produce prolactin in response to hormonal signals and for which dopamine is inhibitory—were Trpc5-negative (*SI Appendix*, Fig. S1*D*).

We further evaluated Trpc5 expression using 3 distinct Trpc5 mutant mouse strains. First, the Trpc5^{L3F1} mouse harboring the *L3F1* mutation containing a floxed exon 4 followed by an expression cassette interrupting the intron sequence between exons 4 and 5 (*SI Appendix*, Fig. S2*A*) (25). The genotype of female mice was either wild type (Trpc5$^{+/+}$), heterozygous (Trpc5$^{+/L3F1}$), or homozygous (Trpc5$^{L3F1/L3F1}$). Second, the Trpc5-E4 mouse in which exon 4 (*E4*) is deleted by Cre-*loxP* recombination (Trpc5-E4$^{-/-}$) (25). Third, the Trpc5-E5 mouse in which exon 5 (*E5*) is deleted by Cre-*loxP* recombination (Trpc5-E5$^{-/-}$) (7). We note that the *Trpc5* gene is located on chromosome X. Experiments of this study focused on female mice with the exception of a few controls that used males.

We assessed Trpc5 expression in these mutant strains using a combination of immunohistochemistry (Fig. 1 *D–F* and *SI Appendix*, Fig. S1 *B–D*), RNAscope fluorescence in situ hybridization (Fig. 1 *G* and *H* and *SI Appendix*, Fig. S2 *D* and *E*), and PCR analyses of genomic DNA (*SI Appendix*, Fig. S2 *A–C*). Together, these experiments revealed that the insertion in the *L3F1* allele results in a hypomorphic mutation that causes Trpc5 knockdown with strongly reduced RNA and protein expression, whereas deletion of *E4* or *E5* resulted in null alleles in which Trpc5 protein expression was not detectable, thus confirming and extending previous reports (7, 25).

Trpc5 Stabilizes Infraslow Oscillations in Th$^+$ ARC Neurons. We next examined the role of Trpc5 in cellular function of Th$^+$ ARC neurons using acute brain slices (26) obtained from adult females of 4 genotypes (Th-tdTomato, Trpc5$^{L3F1/L3F1}$, Trpc5-E4$^{-/-}$, Trpc5-E5$^{-/-}$). We focused on Th$^+$ neurons in the dorsomedial (dm) aspect of ARC that are known to express dopamine (27). These cellular studies are based on analyzing 123 ARC neurons (93 mice) of which 56 were Th$^+$.

Th$^+$ ARC neurons are known for their spontaneous, oscillatory burst firing activity (13, 17, 27). We postulated that the firing properties of these neurons may be altered in Trpc5 mutant mice. We first used Th-tdTomato mice to visualize Th$^+$ ARC neurons in living slices (Fig. 2*A*) and performed whole-cell current clamp recordings in fluorescent Th$^+$ neurons of dmARC to assess their spontaneous firing properties (Fig. 2 *A–D* and *SI Appendix*, Fig. S3). The results confirmed that Th$^+$ ARC neurons show spontaneous rhythmic burst activity, with alternating periods of quiescence (down state) followed by pronounced depolarizations and action potential discharges (up state). The down-state membrane potential (V_D) was −61.7 ± 1.3 mV, with average durations of ~15 s, and the up-state membrane potential (V_U) was −49.1 ± 2.2 mV,

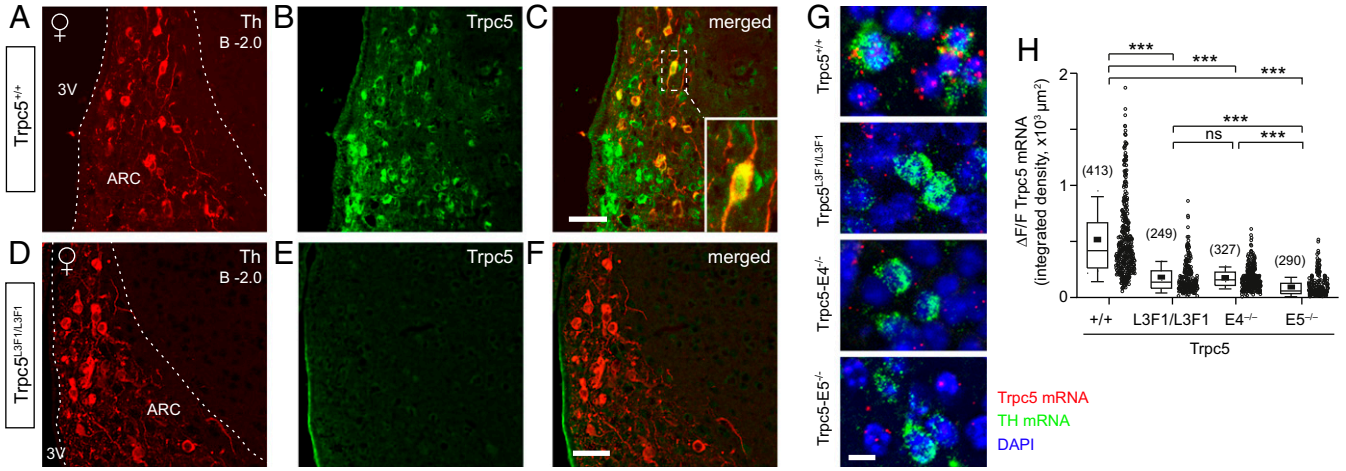

Fig. 1. Th$^+$ ARC neurons express Trpc5. (*A–F*) Immunolabeling of Th (red; *A* and *D*), Trpc5 (green; *B* and *E*) and colocalization of the 2 proteins (merged; *C*, *F*) in Trpc5$^{+/+}$ (*A–C*) and Trpc5$^{L3F1/L3F1}$ (*D–F*) female mice. Merged images show that Th$^+$ ARC neurons express Trpc5 in Trpc5$^{+/+}$ sections (*C* and *Inset*; 271/318 Th$^+$ ARC neurons, $n = 4$ mice; with 85% Th$^+$/Trpc5$^+$ and 15% Th$^+$/Trpc5$^-$ cells), but not in Trpc5$^{L3F1/L3F1}$ females (*F*; 2/426 Th$^+$ ARC neurons, $n = 4$ mice; 0% Trpc5$^+$ cells). Of the Trpc5$^+$ ARC neurons, we found 71% to be Th$^-$ (678/949) and 29% to be Th$^+$ (271/949, $n = 4$ mice). 3V, third ventricle; B, approximate distance (mm) from bregma. (Scale bar, 50 μm.) (*G*) RNAscope fluorescence in situ hybridization using probes directed against the mRNA of *Trpc5* exon 4 (red) or multiple exons of *Th* (green) to identify ARC neurons of Trpc5$^{+/+}$, Trpc5$^{L3F1/L3F1}$, Trpc5-E4$^{-/-}$, and Trpc5-E5$^{-/-}$ females. Cell nuclei were stained with 4′,6-diamidino-2-phenylindole (blue). (Scale bar, 10 μm.) (*H*) Integrated density plots of Trpc5 riboprobe fluorescence measured from Th$^+$ ARC neurons. Values in parentheses indicate the number of TH$^+$ ARC neurons in Trpc5$^{+/+}$, Trpc5$^{L3F1/L3F1}$, Trpc5-E4$^{-/-}$, and Trpc5-E5$^{-/-}$ females ($n = 3$ per genotype). Staining of Trpc5-E4$^{-/-}$ mice can be used to determine background intensity because exon 4 mRNA is absent in these mice. Box plots display the interquartile ranges, median (line), and mean (black square) values with whiskers indicating SD values. Kruskal–Wallis ANOVA: $P < 0.0001$; Mann–Whitney *U* test: ***$P < 0.0001$; ns, $P = 0.14$. Each individual dot represents the integrated density value of a single Th$^+$ ARC neuron. ns, nonsignificant.

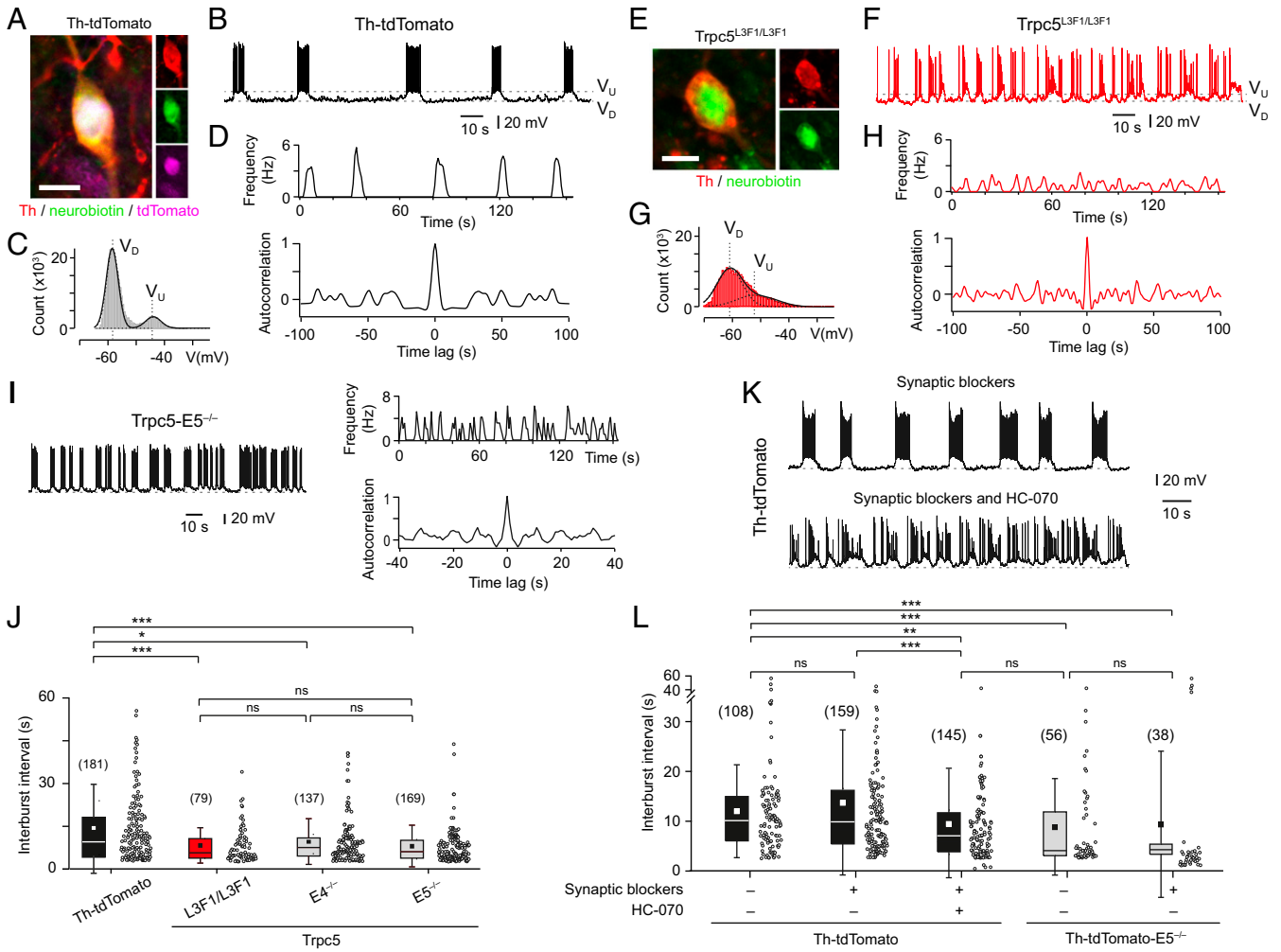

Fig. 2. Trpc5 function is required to stabilize infraslow oscillations in Th$^+$ ARC neurons. (*A*) Example of a neurobiotin-filled (green) tdTomato (magenta) neuron in dmARC from a female Th-tdTomato mouse identified through post hoc immunolabeling as Th$^+$ (red). (*B*) Current clamp recording (I_H = 0 pA) indicating rhythmic activity in a Th$^+$ ARC neuron (Th-tdTomato female). (*C*) Plot of frequency distribution (5-min recording period) of cell shown in *B*. V_D = −58.3 ± 0.03 mV; V_U = −43.4 ± 0.03 mV (mean ± SD). (*D*) Time histogram and normalized ACH (5-min recording period) obtained from the example shown in *B*. (*E*) Post hoc immunofluorescence identifies a neurobiotin-filled dmARC neuron (green) as Th$^+$ (red). (Scale bar, 10 μm.) See also *SI Appendix*, Fig. S3*A*. (*F*) Current-clamp recording showing altered firing pattern of a Th$^+$ ARC neuron (Trpc5$^{L3F1/L3F1}$ female; I_H = 0 pA). (*G*) Frequency distribution plot of 5-min recording shown in *F*. V_D = −60.9 ± 0.3 mV; V_U = −53.0 ± 4.4 mV (mean ± SD). (*H*) Time histogram and normalized ACH obtained from recording shown in *F*. (*I*) Example of a current-clamp recording of a Th$^+$ ARC neuron from a Trpc5-E5$^{-/-}$ female (I_H = 0 pA; V_D = −60 mV), together with time histogram and normalized ACH analyses. RI = 0.13 ± 0.03. (*J*) Interburst interval decreased from 14.1 ± 1.2 s (n = 17 cells, Th-tdTomato) to 8.4 ± 0.7 s (n = 6 cells) in Trpc5$^{L3F1/L3F1}$, 9.7 ± 0.7 s (n = 8 cells) in Trpc5-E4$^{-/-}$, and 8.0 ± 0.6 s (n = 10 cells) in Trpc5-E5$^{-/-}$ Th+ ARC neurons (Kruskal–Wallis ANOVA: $P < 0.001$, Mann–Whitney *U* test: ***$P < 0.001$; *$P < 0.05$; ns, P = 0.06–0.67). Numbers in parentheses indicate the total number of bursts analyzed from at least 3 mice per genotype and plotted as individual dots next to the box plot. (*K*) Current clamp recording (I_H = 0 pA; V_D = −65 mV) of a Th$^+$ ARC neuron (Th-tdTomato) showing rhythmic activity in the presence of antagonists for glutamate and GABA receptors (synaptic blockers, *Upper* trace). Treatment with HC-070 (100 nM) mimicked the effect of the Trpc5 deletion (*Lower* trace). (*L*) Interburst interval in Th$^+$ ARC neurons (Th-tdTomato) did not change in the presence of synaptic blockers (without blockers: 12.0 ± 0.9 s, n = 6 cells; with blockers: 13.7 ± 1.2 s, n = 9 cells), but decreased when treated with HC-070. Interburst interval of HC-070–treated Th$^+$ ARC neurons (9.9 ± 0.9 s, n = 9 cells) was close to the values observed in Trpc5-deficient Th$^+$ ARC neurons (Th-tdTomato-E5$^{-/-}$; without blockers: 8.9 ± 1.3 s, n = 5 cells; with blockers: 9.8 ± 2.5 s, n = 5 cells). Kruskal–Wallis ANOVA: P < 0.001; Mann–Whitney *U* test: ***$P < 0.001$, **$P < 0.01$, and *$P < 0.05$; ns, P = 0.86–0.97. Numbers in parentheses indicate the total number of bursts analyzed from at least 4 mice per genotype and plotted as individual dots next to the box plot. (Scale bars in *A* and *E*, 10 μm.)

with average durations of ∼6 s (n = 17 neurons from 14 mice), all consistent with previous results (13, 17, 27). Normalized autocorrelation histograms (ACHs) demonstrated a striking peak that signifies a predominance of bursting intervals in the responses (Fig. 2*D*). ACH burst refractory period (indicating the silent period following a burst) was 10.5 ± 1.3 s (n = 17 neurons from 14 mice). Th$^+$ ARC neurons had secondary and subsequent peaks indicating oscillatory firing at rates ranging from 0.02 to 0.05 Hz. Thus, wild-type Th$^+$ ARC neurons display pronounced infraslow (28, 29) oscillatory activity.

By contrast, this oscillatory activity was profoundly altered in Th$^+$ ARC neurons from Trpc5$^{L3F1/L3F1}$ females (n = 6 neurons from 6 mice) (Fig. 2 *E–H* and *SI Appendix*, Fig. S3). Th$^+$ ARC neurons were labeled by neurobiotin included in the patch pipette and then underwent post hoc Th immunolabeling (Fig. 2*E* and *SI Appendix*, Fig. S3*A*). The firing activity of these neurons showed several features distinct from wild-type cells such as strikingly reduced interburst intervals and enhanced instantaneous burst frequencies (Fig. 2 *F* and *J* and *SI Appendix*, Fig. S3*C*); increased variability of V_u (Fig. 2 *C* and *G*); and a reduced burst strength (slower voltage ramping from V_D to V_U)

causing a reduction in both depolarization envelope and spike frequency within a burst (Fig. 2 and *SI Appendix*, Fig. S3 *D–F*). Recordings from Th^+ ARC neurons of Trpc5-E4$^{-/-}$ ($n = 8$) and Trpc5-E5$^{-/-}$ ($n = 10$) mice yielded closely similar results (Fig. 2 *I* and *J* and *SI Appendix*, Fig. S3*B*). Together, these observations reveal that Trpc5 determines both the onset phase of a given burst and the interval between bursts. To quantify the regularity of bursting, we calculated a rhythmicity index (RI) (29) and found a 2-fold reduction in Trpc5$^{L3F1/L3F1}$ (RI = 0.16 ± 0.05) versus Th-tdTomato Th^+ ARC neurons (RI = 0.32 ± 0.05). Trpc5-E4$^{-/-}$ and Trpc5-E5$^{-/-}$ Th^+ ARC neurons showed an ∼2.5-fold reduction (Trpc5-E4$^{-/-}$ RI = 0.14 ± 0.05, Trpc5-E5$^{-/-}$ RI = 0.13 ± 0.03).

To exclude synaptic input onto Th^+ ARC neurons as the cause for the change in firing activity, we performed experiments in the presence of pharmacologial antagonists that block glutamate and GABA receptors (*SI Appendix*, *Materials and Methods*). This treatment did not alter the rhythmic properties of Th^+ Arc neurons (Fig. 2 *K* and *L* and *SI Appendix*, Fig. S3*G*), indicating that these oscillations are not of synaptic origin but intrinsically generated by these cells. Furthermore, we applied a potent Trpc5 antagonist, HC-070 (100 nM) (22) and found that acute application of HC-070 mimicked the effects of the Trpc5 deletion in Th^+ Arc neurons (Fig. 2 *K* and *L* and *SI Appendix*, Fig. S3*G*).

Taken together, these results indicate that the presence of Trpc5 in Th^+ ARC neurons stabilizes the regularity of intrinsic rhythmic oscillatory activity and the tendency for infraslow bursting in these cells. Loss of Trpc5 function, either genetically or through acute pharmacological blockade, leads to a strongly reduced interburst interval with an overall increase in firing activity.

Loss of Prolactin-Evoked Tonic Excitation. As part of a short-loop feedback whereby prolactin itself stimulates the secretion of inhibitory dopamine, dopaminergic ARC neurons respond to prolactin with a rise in their firing rate (14, 19). A depolarizing, Trpc-like conductance has been suggested to play a role in this prolactin-evoked excitation (19). We confirmed that Th^+ ARC neurons in slices from female Th-tdTomato mice produce a tonic, long-lasting depolarization accompanied by enhanced action potential firing in response to stimulation with prolactin (500 nM, $n = 10$ mice) (Fig. 3 *A* and *D* and *SI Appendix*, Fig. S4 *C* and *D*). Thus, prolactin exposure switches the membrane potential from a slow rhythmic oscillation to a tonic depolarization in these neurons. By contrast, in Th^+ ARC neurons of Trpc5$^{L3F1/L3F1}$ mice ($n = 5$), the prolactin-evoked tonic excitation was completely absent: Trpc5-deficient cells continued to produce rhythmic activity in the presence of prolactin (Fig. 3 *B* and *E* and *SI Appendix*, Fig. S4 *A–D*). We observed the same results in Trpc5-E4$^{-/-}$ ($n = 3$) and Trpc5-E5$^{-/-}$ ($n = 7$) Th^+ ARC neurons (*SI Appendix*, Fig. S4 *A–D*).

We also confirmed that HC-070 (100 nM), in the presence of glutamate and GABA receptor antagonists, eliminates the prolactin-induced tonic, long-lasting depolarization in Th^+ ARC neurons of Th-tdTomato mice (Fig. 3 *C* and *F* and *SI Appendix*, Fig. S4 *C* and *D*). Therefore, Trpc5 is required for prolactin-evoked, long-lasting plateau potentials in these neurons. Together, the results of Figs. 2 and 3 reveal that Trpc5 deficiency has severe consequences for the firing activity of Th^+ ARC neurons, both under spontaneous conditions and following acute stimulation with prolactin. Trpc5-deficient Th^+ ARC neurons fail to show regular infraslow oscillatory activity, and they fail to respond to acute prolactin stimulation with a long-lasting plateau potential. Our pharmacological experiments show that these effects are due to acute, intrinsic functions of Trpc5 in these cells.

Altered Reproductive Cyclicity, Hypoprolactinemia, and Hormonal Imbalance. Given our results at the cellular level, we reasoned that a loss of Trpc5 may affect hormonal and reproductive

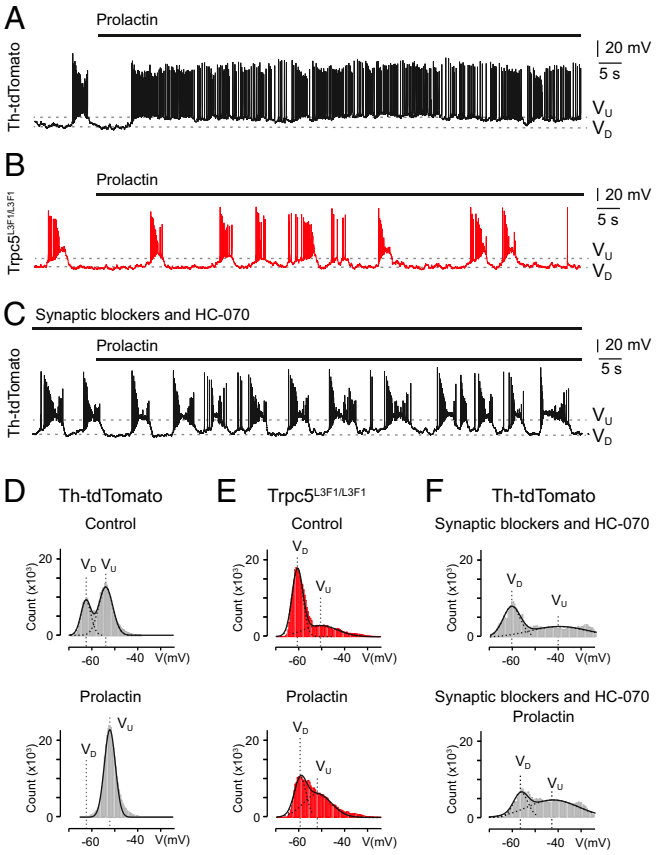

Fig. 3. Trpc5 is required for prolactin-evoked excitation of Th^+ ARC neurons. (*A* and *B*) Prolactin (500 nM) induces a tonic, long-lasting depolarization in Th^+ ARC neurons from female Th-tdTomato mice ($n = 10$), an effect that is absent in Trpc5$^{L3F1/L3F1}$ mice ($n = 5$). (*C*) Loss of prolactin (Prl)-evoked tonic depolarization (Prl, 500 nM) in a Th^+ ARC neuron (Th-tdTomato) after bath application of HC-070 (100 nM) ($n = 6$ cells, 6 Th-tdTomato mice). Experiments were performed in the presence of a synaptic blocker mixture. I_H was 0 pA in all recordings. (*D*) Plot of frequency distribution (recording period, 10 min) of the cell shown in *A* before (control) and during prolactin treatment. Control: $V_D = -62.4 \pm 0.1$ mV; $V_U = -53.9 \pm 0.1$ mV; Prl: $V_U = -52.1 \pm 0.04$ mV (mean ± SD). (*E*) Plot of frequency distribution (recording period, 10 min) of the cell shown in *B* before (control) and during prolactin treatment. Control: $V_D = -60.5 \pm 0.03$ mV; $V_U = -50.1 \pm 0.7$ mV; Prl: $V_D = -59.4 \pm 0.1$ mV; $V_U = -51.9 \pm 0.8$ mV (mean ± SD). (*F*) Plot of frequency distribution (recording period, 10 min) of the cell shown in *C* before (synaptic blockers and HC-070) and during prolactin treatment. Synaptic blockers and HC-070: $V_D = -60.6 \pm 0.1$ mV; $V_U = -39.9 \pm 0.7$ mV; Prl: $V_D = -56.3 \pm 0.1$ mV; $V_U = -46.1 \pm 0.4$ mV (mean ± SD).

function. We next assessed regularity and duration of the 4 phases of the estrous cycle [i.e., metestrus (M), diestrus (D), proestrus (P), and estrus (E)] (Fig. 4 *A–D*). Trpc5$^{+/+}$ mice showed regular cycles with a length of 5.4 ± 0.3 d ($n = 14$ mice). By contrast, Trpc5$^{L3F1/L3F1}$ females had significantly prolonged reproductive cycles (6.5 ± 0.3 d, $n = 28$ mice) (Fig. 4*B*). Prolonged cycle length was also observed in both Trpc5-E4$^{-/-}$ and Trpc5-E5$^{-/-}$ females (Fig. 4*B*). Consistent with these results, Trpc5$^{L3F1/L3F1}$ females experienced all stages of the murine reproductive cycle, but their cycles were irregular, with signs of oligo-ovulation based on vaginal cytology. Trpc5-deficient females showed less frequent episodes of estrus (fraction of time spent in estrus during a cycle: Trpc5$^{+/+}$: 0.26 ± 0.03, $n = 14$ mice; Trpc5$^{L3F1/L3F1}$: 0.17 ± 0.01, $n = 28$ mice) and had longer phases of diestrus (Trpc5$^{+/+}$: 0.38 ± 0.03; Trpc5$^{L3F1/L3F1}$: 0.47 ± 0.03) (Fig. 4 *A*, *C*, and *D*). Furthermore, the duration of diestrus was prolonged, from 2 to 4 d in Trpc5$^{+/+}$ to 2 to 8 d in Trpc5$^{L3F1/L3F1}$ females.

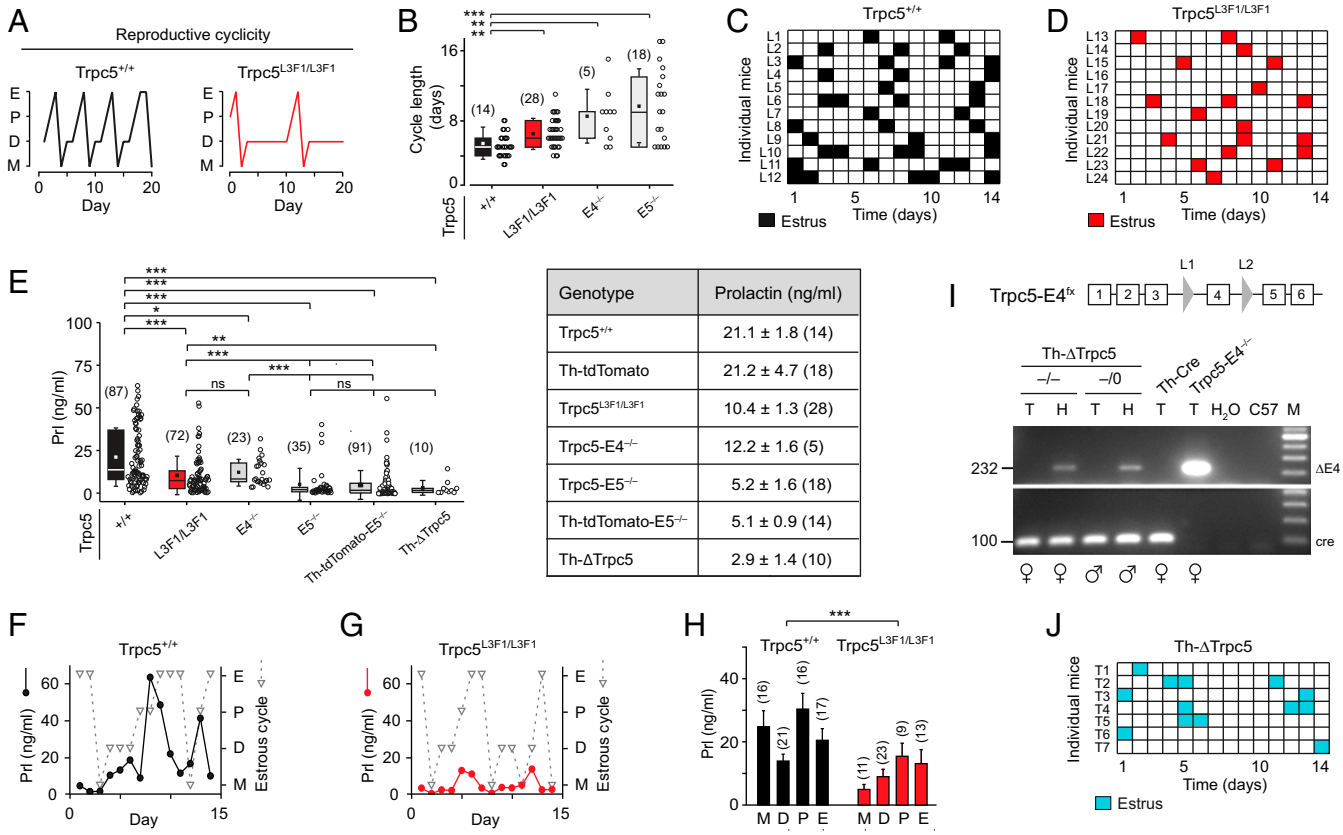

Genotype	Prolactin (ng/ml)
$Trpc5^{+/+}$	21.1 ± 1.8 (14)
Th-tdTomato	21.2 ± 4.7 (18)
$Trpc5^{L3F1/L3F1}$	10.4 ± 1.3 (28)
Trpc5-E4$^{-/-}$	12.2 ± 1.6 (5)
Trpc5-E5$^{-/-}$	5.2 ± 1.6 (18)
Th-tdTomato-E5$^{-/-}$	5.1 ± 0.9 (14)
Th-ΔTrpc5	2.9 ± 1.4 (10)

Fig. 4. Hypoprolactinemia and impaired reproductive cyclicity in Trpc5-deficient mice. (*A*) Examples of reproductive cycles from 7- to 12-wk-old sexually naive female $Trpc5^{+/+}$ and $Trpc5^{L3F1/L3F1}$ mice evaluated by daily vaginal cytology. $Trpc5^{L3F1/L3F1}$ females display irregular reproductive cycles with longer dwell times in diestrus. (*B*) Prolonged cycle length in sexually naive Trpc5-deficient females. $Trpc5^{+/+}$: 5.4 ± 0.3 d, $n = 14$ mice; $Trpc5^{L3F1/L3F1}$: 6.5 ± 0.3 d, $n = 28$ mice; Trpc5-E4$^{-/-}$: 8.5 ± 1.0 d, $n = 5$ mice; Trpc5-E5$^{-/-}$: 9.7 ± 1.0 d, $n = 18$ mice; Kruskal–Wallis ANOVA: $P < 0.001$; Mann–Whitney *U* test: ***$P < 0.001$, **$P < 0.01$. Box plots display the interquartile ranges, median (line), and mean (black/white squares) values with whiskers indicating SD values. Each dot represents a given estrous cycle. (*C* and *D*) Checkerboard plots showing daily evaluations of vaginal smears in individual $Trpc5^{+/+}$ (*C*) and $Trpc5^{L3F1/L3F1}$ (*D*) females for the occurrence of estrus (filled squares). Trpc5-deficient females showed a reduced incidence of estrus. (*E*) Trpc5-deficient female mice harboring a global or conditional Trpc5 deletion exhibit strongly reduced Prl levels. Number of independent measurements from at least 5 mice per genotype is indicated above each box plot (Kruskal–Wallis ANOVA: $P < 0.001$; Mann–Whitney *U* test: ***$P < 0.001$; **$P < 0.01$; *$P < 0.05$; ns, $P = 0.08 - 0.61$). See table on *Right* for mean ± SEM values and total number of mice in parentheses. (*F–H*) Daily analyses of prolactin levels during reproductive cycles of individual $Trpc5^{+/+}$ (*F*) and $Trpc5^{L3F1/L3F1}$ (*G*) mice and the group data (*H*) show that $Trpc5^{L3F1/L3F1}$ females display prolactin surges but that overall prolactin levels are reduced. Prolactin levels are significantly diminished in $Trpc5^{L3F1/L3F1}$ females at all stages of the reproductive cycle ($Trpc5^{+/+}$: M, Prl, 24.7 ± 5.0 ng/mL; D, Prl, 13.9 ± 2.2 ng/mL; P, Prl, 30.2 ± 5.0 ng/mL; E, Prl, 20.4 ± 3.7 ng/mL; $Trpc5^{L3F1/L3F1}$: M, Prl, 4.1 ± 1.3 ng/mL; D, Prl, 8.2 ± 2.0 ng/mL; P, Prl, 15.2 ± 3.8 ng/mL; E, Prl, 11.1 ± 3.4 ng/mL; Kruskal–Wallis ANOVA: $P < 0.001$; Mann–Whitney *U* test: ***$P < 0.001$). Number of independent measurements from at least 5 mice is indicated above each bar. (*I*) Generation and validation of Th-ΔTrpc5 conditional knockout mice. Mice carrying the *Trpc5-E4*^{fx} allele (*Top*), in which exon 4 (E4) is flanked by *loxP* sites (gray triangles, L1–L2), were mated with Th-Cre transgenic mice. The resulting mice carry a retained *loxP* site between exons 3 and 5 after deletion of exon 4. Mice were verified by PCR using genomic DNA prepared from tail (T) or hypothalamus (H), followed by sequencing of PCR products. Gel electrophoresis illustrates that genomic PCR amplifies the truncated region (232 bp) only from hypothalamus but not from tail of homozygous females (–/–) and hemizygous (–/0) males. Positive control: tail genomic DNA from Trpc4-E4$^{-/-}$ mice; negative controls: H_2O (water template) and C57BL6/N genomic DNA (C57). PCR product sizes in base pairs are as indicated at the left. Sequencing confirmed the deletion of the exon 4 region in the hypothalamus of Th-ΔTrpc5 mice. (*J*) Checkerboard plots showing reproductive cycles of Th-ΔTrpc5 females ($n = 7$) reveal irregular, less frequent, and delayed estrus episodes in conditional Trpc5 knockout mice.

Reproductive cycles with long luteal phases (M and D) can be indicative of altered prolactin levels (30). We determined the concentrations of several pituitary hormones in blood serum obtained from sexually naive females (6–16 wk old). $Trpc5^{L3F1/L3F1}$ females had severely diminished prolactin levels compared with $Trpc5^{+/+}$ females (Fig. 4*E*; $Trpc5^{+/+}$: Prl = 21.1 ± 1.8 ng/mL; $Trpc5^{L3F1/L3F1}$: Prl = 10.4 ± 1.3 ng/mL). This effect was also clearly evident in Trpc5-E4$^{-/-}$, Trpc5-E5$^{-/-}$, and Th-tdTomato-E5$^{-/-}$ females (Fig. 4*E*). Thus, Trpc5 deficiency causes pronounced hypoprolactinemia. By performing daily blood collections and related hormone measurements at known cycle stages of individual mice ($Trpc5^{+/+}$ and $Trpc5^{L3F1/L3F1}$ females) and plotting the data over time, we found that $Trpc5^{L3F1/L3F1}$ females still showed prolactin surges. However, the peak values of these surges were significantly reduced during all cycle stages compared with $Trpc5^{+/+}$ mice (Fig. 4 *F–H*).

To obtain evidence for cellular specificity of these major systemic phenotypes, we created a conditional knockout model. We used the Cre-*loxP* system (31–33) to delete the channel only in Th^+ cells, ruling out a potential involvement of kisspeptin and POMC neurons or of pituitary gonadotrophs (34). We crossed Th-Cre mice with mice harboring a floxed Trpc5 allele, Trpc5-E4$^{fx/fx}$ (25). Offspring from this cross will be referred to as Th-Cre::Trpc5-E4$^{fx/fx}$, or Th-ΔTrpc5. PCR of genomic DNA and sequence analyses of the products obtained confirmed tissue-specific and Cre-dependent deletion of exon 4 in the hypothalamus of male or female Th-ΔTrpc5 mice (Fig. 4*I*). Importantly, prolactin levels in sexually naive Th-ΔTrpc5 female mice (6–14 wk old, $n = 10$) were profoundly reduced compared with

Trpc5$^{+/+}$ and Th-tdTomato females (Prl = 2.9 ± 1.4 ng/mL; Fig. 4*E*), indicating hypoprolactinemia in the conditional knockout mice. Furthermore, reproductive cycle measurements of Th-ΔTrpc5 females (n = 7) revealed irregular, less frequent, and delayed episodes of estrus (Fig. 4*J*), very similar to the effect observed in global Trpc5-deficient females. Therefore, hypoprolactinemia—combined with irregular reproductive cyclicity—occurred not only in global Trpc5-deficient mice but also after conditional Trpc5 deletion under the control of the *Th* promoter.

Taken together, these results are consistent with altered release of dopamine at the median eminence during the entire reproductive cycle which, in turn, could also affect the release of gonadotropin-releasing hormone that controls secretion of luteinizing hormone (LH) and follicle stimulating hormone (FSH). Indeed, we found significantly increased LH/FSH ratios during the entire ovulatory period in Trpc5$^{L3F1/L3F1}$ females (*SI Appendix*, Fig. S5*A*). LH surges occurred in all Trpc5$^{+/+}$ and Trpc5$^{L3F1/L3F1}$ females, but in some Trpc5$^{L3F1/L3F1}$ females LH peaks were delayed and appeared during the estrous stage (*SI Appendix*, Fig. S5*B*). These results and the vaginal cytology (*Materials and Methods*) predict that Trpc5$^{L3F1/L3F1}$ females should ovulate normally. The increased LH/FSH ratios can be explained by significantly lowered FSH levels (*SI Appendix*, Fig. S5*C*). The LH/FSH imbalance could lead to the presence of polycystic ovaries, but we found no defects in ovary morphology (35) in Trpc5$^{L3F1/L3F1}$ mice (*SI Appendix*, Fig. S5 *D* and *E*).

Impaired Reproductive Capabilities. Having shown that Trpc5 deficiency is associated with hypoprolactinemia, we next assessed reproductive capabilities of Trpc5-deficient females (Fig. 5). Reduced levels of prolactin could affect embryo implantation (nidation) and cause pregnancy failure. Indeed, we found that the relative fecundity—a measure for the actual reproductive performance—of individual Trpc5$^{L3F1/L3F1}$ females was strongly reduced compared with Trpc5$^{+/+}$ females, by as much as 7.7-fold (Fig. 5*A*). This effect was also observed in both Trpc5-E4$^{-/-}$ and Trpc5-E5$^{-/-}$ females (Fig. 5*A*). Furthermore, the percentage of productive matings, number of litters, and litter size were all significantly reduced whereas the litter interval was significantly prolonged in Trpc5$^{L3F1/L3F1}$ females (Fig. 5 *B*–*E*). Closely similar results were obtained in Trpc5-E4$^{-/-}$ and Trpc5-E5$^{-/-}$ females, although with quantitative differences between the genotypes (Fig. 5 *B*–*E*). Trpc5 mutant newborn pups (Trpc5$^{L3F1/L3F1}$, Trpc5-E4$^{-/-}$, or Trpc5-E5$^{-/-}$) showed normal body weights, and their weight gain over time was normal compared with controls (*SI Appendix*, Fig. S5 *F* and *G*), consistent with previous results (6).

Thus, Trpc5 mutant females display severe impairments in their reproductive capabilities: Trpc5-deficient breeding pairs can be fertile, but almost 50% of matings fail to become pregnant and do not produce any offspring. In case of productive matings, a temporal delay in the occurrence of pregnancy and a reduced number of offspring is observed, consistent with low prolactin levels and defects in nidation.

Discussion

Hyperprolactinemia is a major neuroendocrine-related cause of reproductive disturbances in both men and women (12, 36), but comparatively little is still known about the underlying causes of prolactin deficiency—hypoprolactinemia (37). To our knowledge, no gene defects in any ion channel that cause hypoprolactinemia have been described thus far. By analyzing mouse models harboring targeted mutations in the *Trpc5* cation channel gene, we found that the presence of Trpc5 is a major determinant of circulating prolactin levels and prolactin homeostasis in female mice. These studies provide substantial evidence that Trpc5 deficiency causes profound hypoprolactinemia that, in turn, is associated with irregular reproductive cyclicity, gonadotropin imbalance, and impaired reproductive capabilities.

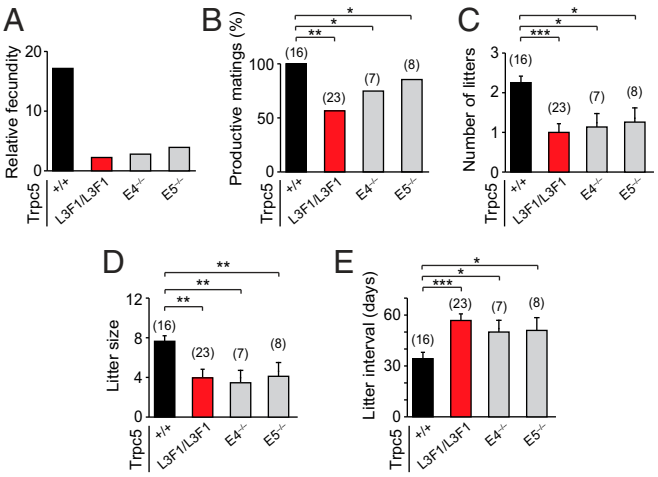

Fig. 5. Impaired reproductive capabilities in Trpc5-deficient mice. (*A*) Relative fecundity values are strikingly reduced in Trpc5-deficient mice versus Trpc5$^{+/+}$ breedings (Trpc5$^{+/+}$, 17.2; Trpc5$^{L3F1/L3F1}$, 2.2; Trpc5-E4$^{-/-}$, 2.8; Trpc5-E5$^{-/-}$, 3.9). Sexually mature (8–12 wk old) female and male mice were kept as single mating pairs over a 3-mo test period. Relative fecundity = (productive matings) × (litter size) × (number of litters). (*B*) Trpc5-deficient mating pairs can be fertile, but breeding success (percentage of productive matings) is diminished. Productive matings: Trpc5$^{+/+}$, 16/16; Trpc5$^{L3F1/L3F1}$, 13/23; Trpc5-E4$^{-/-}$, 5/7; Trpc5-E5$^{-/-}$, 6/8; $^{**}P < 0.01$; $^{*}P < 0.05$. (*C*–*E*) Number of litters (*C*) and litter size (*D*) are reduced whereas the interval of pregnancies (*E*) increased. (*C*) Number of litters, Trpc5$^{+/+}$: 2.3 ± 0.2; Trpc5$^{L3F1/L3F1}$: 1.0 ± 0.2; Trpc5-E4$^{-/-}$: 1.1 ± 0.3; Trpc5-E5$^{-/-}$: 1.3 ± 0.4; Kruskal–Wallis ANOVA: $P < 0.01$. (*D*) Litter size, Trpc5$^{+/+}$: 7.7 ± 0.56; Trpc5$^{L3F1/L3F1}$: 3.9 ± 0.9; Trpc5-E4$^{-/-}$: 3.4 ± 1.3; Trpc5-E5$^{-/-}$: 4.2 ± 1.3; Kruskal-Wallis ANOVA: $P < 0.05$. (*E*) Litter interval, Trpc5$^{+/+}$: 34.3 ± 3.8 d; Trpc5$^{L3F1/L3F1}$: 56.8 ± 3.9 d; Trpc5-E4$^{-/-}$: 50.0 ± 7.1 d; Trpc5-E5$^{-/-}$: 51.0 ± 7.3 d; Kruskal–Wallis ANOVA: $P < 0.01$. Mann–Whitney *U* test: $^{*}P < 0.05$; $^{**}P < 0.01$; $^{***}P < 0.001$. Litter size was determined at postnatal day 0–1. Numbers in parentheses indicate number of female mice.

Thus, we have revealed an unexpected role of Trpc5 in the maintenance of normal serum prolactin levels. As prolactin is now recognized as a pleiotrophic hormone with one of the widest ranges of physiological actions of any extracellular signaling molecule in the body (14, 16), these results should impact a broad range of biological functions and phenotypic traits.

At the cellular level, our studies identify Trpc5 as a previously unknown determinant of the physiology of Th^{+} neurons of dmARC. As dopamine released from these neurons provides inhibitory control over the secretion of prolactin by lactotrophs, there is a direct link between the function of dopamine ARC neurons and pituitary prolactin secretion (12, 14). Our studies show that Trpc5 deficiency has severe consequences for the firing activity of Th^{+} ARC neurons, both under spontaneous conditions and following acute stimulation with prolactin. We found that the presence of Trpc5 is critically required for stabilizing infraslow membrane potential oscillations (Fig. 2), which are a highly stereotypic feature of these neurons under normal conditions (13). Furthermore, our results indicate that a loss of Trpc5 increases the overall activity of spontaneously spiking Th^{+} ARC neurons. We also demonstrate that Trpc5-deficient Th^{+} ARC neurons fail to respond to acute prolactin stimulation with a long-lasting plateau potential (Fig. 3), suggesting that the short-loop feedback circuit mediating regulation of dopamine release should be impaired. Importantly, these genetic effects persist in the presence of blockers that uncouple the synaptic network, indicating that they are intrinsic to the Th^{+} ARC neurons and that they can be mimicked by acute application of the Trpc5 antagonist HC-070. Therefore, these experiments have identified a role for Trpc5 in the function of dopamine ARC neurons and, together with previous findings (7, 38), they

support a more general function for Trpc5 in the generation of membrane potential oscillations and long-lasting plateau potentials in the CNS.

One possible mechanism of how Trpc5 could stabilize the infraslow oscillations of Th^+ ARC neurons is through the generation of long-lasting Ca^{2+} plateaus, which, in turn, could activate hyperpolarizing conductances that determine the interburst intervals. Studies in dopamine midbrain neurons have revealed a complex interplay between several types of ion channels in the generation of rhythmic activity including small-conductance Ca^{2+}-dependent K^+ channels, ATP-sensitive K^+ channels, and hyperpolarization-activated cyclic nucleotide-gated cation channels (39–43). Similar mechanisms may also be involved in the rhythmic activity of Th^+ ARC neurons, and several types of K^+ currents have already been identified in dopamine ARC neurons (19). It will also be important to determine what activates Trpc5 under resting conditions. The discovery of photoswitchable diacylglycerols that enable optical activation and deactivation of diacylglycerol-sensitive TRP channels in mammalian tissue slices (44) should aid in exploring these questions.

To provide cellular specificity for the major systemic phenotypes—prolactin deficiency and irregular reproductive cyclicity—we generated a conditional knockout model in which Trpc5 is ablated under the control of the *Th* promoter, referred to as Th-ΔTrpc5 mice (Fig. 4). This approach ruled out a potential involvement of $Trpc5^+/Th^-$ cells such as POMC and kisspeptin neurons or of pituitary gonadotrophs. These experiments provide clear evidence that prolactin levels were also profoundly reduced in female Th-ΔTrpc5 mice. Furthermore, the reproductive cycles of Th-ΔTrpc5 females were irregular, less frequent, and delayed, thereby mimicking the effects of a global Trpc5 deficiency. Thus, hypoprolactinemia combined with irregular reproductive cyclicity occurred not only in global Trpc5-deficient mice but also after conditional Trpc5 deletion under the control of the *Th* promoter. Within the reproductive axis, we note that Trpc5 protein expression was absent in lactotrophs of the anterior pituitary (*SI Appendix*, Fig. S1). In gonadotrophs, *Trpc5* expression has been observed only in juvenile females (34). Together with our observations of normal weight gain and occurrence of LH surges in the Trpc5 mutant mice (*SI Appendix*, Fig. S5), our results argue that the phenotypes that we describe should be caused predominantly by an altered function of Th^+ ARC neurons.

We therefore propose a model in which the presence of Trpc5 in Th^+ ARC neurons influences prolactin homeostasis. More specifically, we hypothesize that the altered firing patterns observed in Trpc5-deficient Th^+ ARC neurons should influence dopamine release at the median eminence and that the hyperprolactinemia phenotype may result primarily from these effects. The observed increase in instantaneous burst frequency after Trpc5 deletion could result in enhanced release of dopamine, thereby leading to prolactin deficiency. A recent report in male mice analyzing dopamine release dynamics at the median eminence using optogenetic stimulation and fast-scan voltammetry showed that dopamine output is maximal at action potential frequencies near 10 Hz within a single 5-s burst (21). However, these experiments did not test the impact of altered burst intervals within the time range of our findings. Future studies will be required to examine the consequences of Trpc5 deficiency on dopamine release from Th^+ ARC neurons (17, 18, 20) in female mice, also taking into account the role of feedback control mechanisms in the lactotrophic axis (19). The use of recently developed, genetically encoded dopamine sensors (45, 46) will provide innovative approaches to investigate these questions in the future.

In summary, our studies open the door to begin to determine whether mutations in the human *TRPC5* gene (47) would equally be associated with prolactin deficiency. Thus far, no clear TRPC5 channelopathies, either congenital or acquired, have been identified to underlie dysfunction and disease in humans (48). Such initiatives could potentially lead to new treatment options for reproductive disorders and other malfunctions associated with defective prolactin homeostasis.

Materials and Methods

Animal care and experimental procedures were performed in accordance with the guidelines established by the animal welfare committee of Saarland University. Unless otherwise stated, data are expressed as means ± SEM. Further details on mutant mice, immunohistochemistry, RNAscope in situ hybridization, hormonal testing, assessment of reproductive capability, electrophysiology, statistics, and other experiments are provided in *SI Appendix, Materials and Methods*.

ACKNOWLEDGMENTS. We thank Christian Eickmeier (Boehringer Ingelheim) for generously providing the HC-070 antagonist; Monika Vorndran and Petra Hammes for help with genotyping; and Lisa-Marie Knieriemen for assistance with blood sampling and reproductive cycle measurements. Veit Flockerzi provided helpful discussions on this project. This work was supported by Deutsche Forschungsgemeinschaft (DFG) Grant Sonderforschungsbereich-Transregio TRR 152, project no. 239283807 (to P.W., M.F., F.Z., and T.L.-Z.); Sonderforschungsbereich 894 (to F.Z. and T.L.-Z.); Sonderforschungsbereich 1118 (to M.F.); DFG Instrumentation Grant INST 256/427-1 FUGB (to T.L.-Z.); and the Volkswagen Foundation (to T.L.-Z.).

1. D. E. Clapham, C. Montell, G. Schultz, D. Julius; International Union of Pharmacology, International union of pharmacology. XLIII. Compendium of voltage-gated ion channels: Transient receptor potential channels. *Pharmacol. Rev.* **55**, 591–596 (2003).
2. K. Venkatachalam, C. Montell, TRP channels. *Annu. Rev. Biochem.* **76**, 387–417 (2007).
3. A. Zholos, "TRPC5" in *Mammalian Transient Receptor Potential (TRP) Cation Channels*, B. Nilius, V. Flockerzi, Eds. (Springer, Berlin, Heidelberg, 2014), vol. 1, pp. 129–156.
4. U. Storch *et al.*, Dynamic NHERF interaction with TRPC4/5 proteins is required for channel gating by diacylglycerol. *Proc. Natl. Acad. Sci. U.S.A.* **114**, E37–E46 (2017).
5. Y. Zhou *et al.*, A small-molecule inhibitor of TRPC5 ion channels suppresses progressive kidney disease in animal models. *Science* **358**, 1332–1336 (2017).
6. A. Riccio *et al.*, Essential role for TRPC5 in amygdala function and fear-related behavior. *Cell* **137**, 761–772 (2009).
7. K. D. Phelan *et al.*, Canonical transient receptor channel 5 (TRPC5) and TRPC1/4 contribute to seizure and excitotoxicity by distinct cellular mechanisms. *Mol. Pharmacol.* **83**, 429–438 (2013).
8. A. Greka, B. Navarro, E. Oancea, A. Duggan, D. E. Clapham, TRPC5 is a regulator of hippocampal neurite length and growth cone morphology. *Nat. Neurosci.* **6**, 837–845 (2003).
9. J. Bröker-Lai *et al.*, Heteromeric channels formed by TRPC1, TRPC4 and TRPC5 define hippocampal synaptic transmission and working memory. *EMBO J.* **36**, 2770–2789 (2017).
10. Y. Gao *et al.*, TrpC5 mediates acute leptin and serotonin effects via pomc neurons. *Cell Rep.* **18**, 583–592 (2017).
11. J. Qiu, E. J. Wagner, O. K. Rønnekleiv, M. J. Kelly, Insulin and leptin excite anorexigenic pro-opiomelanocortin neurones via activation of TRPC5 channels. *J. Neuroendocrinol.* **30**, e12501 (2018).
12. N. Ben-Jonathan, R. Hnasko, Dopamine as a prolactin (PRL) inhibitor. *Endocr. Rev.* **22**, 724–763 (2001).
13. D. J. Lyons, C. Broberger, TIDAL WAVES: Network mechanisms in the neuroendocrine control of prolactin release. *Front. Neuroendocrinol.* **35**, 420–438 (2014).
14. D. R. Grattan, 60 years of neuroendocrinology: The hypothalamo-prolactin axis. *J. Endocrinol.* **226**, T101–T122 (2015).
15. A. Björklund, S. B. Dunnett, Dopamine neuron systems in the brain: An update. *Trends Neurosci.* **30**, 194–202 (2007).
16. M. E. Freeman, B. Kanyicska, A. Lerant, G. Nagy, Prolactin: Structure, function, and regulation of secretion. *Physiol. Rev.* **80**, 1523–1631 (2000).
17. D. J. Lyons, E. Horjales-Araujo, C. Broberger, Synchronized network oscillations in rat tuberoinfundibular dopamine neurons: Switch to tonic discharge by thyrotropin-releasing hormone. *Neuron* **65**, 217–229 (2010).
18. A. N. van den Pol, Excitatory neuromodulator reduces dopamine release, enhancing prolactin secretion. *Neuron* **65**, 147–149 (2010).
19. D. J. Lyons, A. Hellysaz, C. Broberger, Prolactin regulates tuberoinfundibular dopamine neuron discharge pattern: Novel feedback control mechanisms in the lactotrophic axis. *J. Neurosci.* **32**, 8074–8083 (2012).
20. N. Romanò, A. Guillou, D. J. Hodson, A. O. Martin, P. Mollard, Multiple-scale neuroendocrine signals connect brain and pituitary hormone rhythms. *Proc. Natl. Acad. Sci. U.S.A.* **114**, 2379–2382 (2017).

21. S. Stagkourakis, J. Dunevall, Z. Taleat, A. G. Ewing, C. Broberger, Dopamine release dynamics in the tuberoinfundibular dopamine system. *J. Neurosci.* **39**, 4009–4022 (2019).
22. S. Just *et al*., Treatment with HC-070, a potent inhibitor of TRPC4 and TRPC5, leads to anxiolytic and antidepressant effects in mice. *PLoS One* **13**, e0191225 (2018).
23. J. M. Savitt, S. S. Jang, W. Mu, V. L. Dawson, T. M. Dawson, Bcl-x is required for proper development of the mouse substantia nigra. *J. Neurosci.* **25**, 6721–6728 (2005).
24. L. Madisen *et al*., A robust and high-throughput Cre reporting and characterization system for the whole mouse brain. *Nat. Neurosci.* **13**, 133–140 (2010).
25. T. Xue *et al*., Melanopsin signalling in mammalian iris and retina. *Nature* **479**, 67–73 (2011).
26. C. Schauer *et al*., Hypothalamic gonadotropin-releasing hormone (GnRH) receptor neurons fire in synchrony with the female reproductive cycle. *J. Neurophysiol.* **114**, 1008–1021 (2015).
27. X. Zhang, A. N. van den Pol, Dopamine/tyrosine hydroxylase neurons of the hypothalamic arcuate nucleus release GABA, communicate with dopaminergic and other arcuate neurons, and respond to dynorphin, met-enkephalin, and oxytocin. *J. Neurosci.* **35**, 14966–14982 (2015).
28. M. Gorin *et al*., Interdependent conductances drive infraslow intrinsic rhythmogenesis in a subset of accessory olfactory bulb projection neurons. *J. Neurosci.* **36**, 3127–3144 (2016).
29. A. Zylbertal, Y. Yarom, S. Wagner, Synchronous infra-slow bursting in the mouse accessory olfactory bulb emerge from interplay between intrinsic neuronal dynamics and network connectivity. *J. Neurosci.* **37**, 2656–2672 (2017).
30. S. Hansen, P. Södersten, P. Eneroth, Mechanisms regulating hormone release and the duration of dioestrus in the lactating rat. *J. Endocrinol.* **99**, 173–180 (1983).
31. J. Weiss *et al*., Loss-of-function mutations in sodium channel $Na_v1.7$ cause anosmia. *Nature* **472**, 186–190 (2011).
32. P. Chamero *et al*., G protein G(α)o is essential for vomeronasal function and aggressive behavior in mice. *Proc. Natl. Acad. Sci. U.S.A.* **108**, 12898–12903 (2011).
33. A.-C. Trouillet *et al*., Central role of G protein Gαi2 and $G\alpha i2^{+}$ vomeronasal neurons in balancing territorial and infant-directed aggression of male mice. *Proc. Natl. Acad. Sci. U.S.A.* **116**, 5135–5143 (2019).
34. A. Beck *et al*., Functional characterization of transient receptor potential (TRP) channel C5 in female murine gonadotropes. *Endocrinology* **158**, 887–902 (2017).
35. L. Oboti *et al*., A wide range of pheromone-stimulated sexual and reproductive behaviors in female mice depend on G protein Gαo. *BMC Biol.* **12**, 31 (2014).
36. U. B. Kaiser, Hyperprolactinemia and infertility: New insights. *J. Clin. Invest.* **122**, 3467–3468 (2012).
37. S. Iwama, C. K. Welt, C. J. Romero, S. Radovick, P. Caturegli, Isolated prolactin deficiency associated with serum autoantibodies against prolactin-secreting cells. *J. Clin. Endocrinol. Metab.* **98**, 3920–3925 (2013).
38. C. Tai, D. J. Hines, H. B. Choi, B. A. MacVicar, Plasma membrane insertion of TRPC5 channels contributes to the cholinergic plateau potential in hippocampal CA1 pyramidal neurons. *Hippocampus* **21**, 958–967 (2011).
39. J. Wolfart, J. Roeper, Selective coupling of T-type calcium channels to SK potassium channels prevents intrinsic bursting in dopaminergic midbrain neurons. *J. Neurosci.* **22**, 3404–3413 (2002).
40. H. Neuhoff, A. Neu, B. Liss, J. Roeper, $I_{(h)}$ channels contribute to the different functional properties of identified dopaminergic subpopulations in the midbrain. *J. Neurosci.* **22**, 1290–1302 (2002).
41. S. N. Blythe, D. Wokosin, J. F. Atherton, M. D. Bevan, Cellular mechanisms underlying burst firing in substantia nigra dopamine neurons. *J. Neurosci.* **29**, 15531–15541 (2009).
42. J. Schiemann *et al*., K-ATP channels in dopamine substantia nigra neurons control bursting and novelty-induced exploration. *Nat. Neurosci.* **15**, 1272–1280 (2012).
43. E. Dragicevic, J. Schiemann, B. Liss, Dopamine midbrain neurons in health and Parkinson's disease: Emerging roles of voltage-gated calcium channels and ATP-sensitive potassium channels. *Neuroscience* **284**, 798–814 (2015).
44. T. Leinders-Zufall *et al*., PhoDAGs enable optical control of diacylglycerol-sensitive transient receptor potential channels. *Cell Chem. Biol.* **25**, 215–223.e3 (2018).
45. T. Patriarchi *et al*., Ultrafast neuronal imaging of dopamine dynamics with designed genetically encoded sensors. *Science* **360**, eaat4422 (2018).
46. F. Sun *et al*., A genetically encoded fluorescent sensor enables rapid and specific detection of dopamine in flies, fish, and mice. *Cell* **174**, 481–496.e19 (2018).
47. C. Mignon-Ravix *et al*., Intragenic rearrangements in X-linked intellectual deficiency: Results of a-CGH in a series of 54 patients and identification of TRPC5 and KLHL15 as potential XLID genes. *Am. J. Med. Genet. A.* **164A**, 1991–1997 (2014).
48. B. Nilius, G. Owsianik, T. Voets, J. A. Peters, Transient receptor potential cation channels in disease. *Physiol. Rev.* **87**, 165–217 (2007).